

The Diffuse Light Envelope of Luminous Red Galaxies

Y. LEUNG,¹ Y. ZHANG,² B. YANNY,² K. HERNER,² J. ANNIS,² A. PALMESE,^{2,1} H. SAMPAIO-SANTOS,^{3,4} V. STRAZZULLO,⁵
M. AGUENA,^{4,6} S. ALLAM,² S. AVILA,⁷ E. BERTIN,^{8,9} S. BHARGAVA,¹⁰ D. BROOKS,¹¹ D. L. BURKE,^{12,13} A. CARNERO ROSELL,^{14,4}
M. CARRASCO KIND,^{15,16} J. CARRETERO,¹⁷ M. COSTANZI,^{18,19} L. N. DA COSTA,^{3,4} S. DESAI,²⁰ H. T. DIEHL,² P. DOEL,¹¹
T. F. EIFLER,^{21,22} S. EVERETT,²³ B. FLAUGHER,² J. FRIEMAN,^{1,2} J. GARCÍA-BELLIDO,⁷ E. GAZTANAGA,^{24,25} D. GRUEN,^{12,13,26}
R. A. GRUENL,^{16,15} J. GSCHWEND,^{4,3} G. GUTIERREZ,² K. HONSCHIED,^{27,28} D. J. JAMES,²⁹ A. G. KIM,³⁰ K. KUEHN,^{31,32}
N. KUROPATKIN,² M. LIMA,^{6,4} M. A. G. MAIA,^{4,3} R. MIQUEL,^{33,17} R. L. C. OGANDO,^{4,3} F. PAZ-CHINCHÓN,^{15,34} A. A. PLAZAS,³⁵
A. K. ROMER,¹⁰ A. ROODMAN,^{12,13} E. S. RYKOFF,^{13,12} E. SANCHEZ,¹⁴ V. SCARPINE,² M. SCHUBNELN,³⁶ S. SERRANO,^{24,25}
I. SEVILLA-NOARBE,¹⁴ M. SMITH,³⁷ E. SUCHYTA,³⁸ M. E. C. SWANSON,¹⁵ AND T. N. VARGA^{39,40}

¹Kavli Institute for Cosmological Physics, University of Chicago, Chicago, IL 60637, USA

²Fermi National Accelerator Laboratory, P. O. Box 500, Batavia, IL 60510, USA

³Observatório Nacional, Rua Gal. José Cristino 77, Rio de Janeiro, RJ - 20921-400, Brazil

⁴Laboratório Interinstitucional de e-Astronomia - LIneA, Rua Gal. José Cristino 77, Rio de Janeiro, RJ - 20921-400, Brazil

⁵Faculty of Physics, Ludwig-Maximilians-Universität, Scheinerstr. 1, 81679 Munich, Germany

⁶Departamento de Física Matemática, Instituto de Física, Universidade de São Paulo, CP 66318, São Paulo, SP, 05314-970, Brazil

⁷Instituto de Física Teórica UAM/CSIC, Universidad Autónoma de Madrid, 28049 Madrid, Spain

⁸Sorbonne Universités, UPMC Univ Paris 06, UMR 7095, Institut d'Astrophysique de Paris, F-75014, Paris, France

⁹CNRS, UMR 7095, Institut d'Astrophysique de Paris, F-75014, Paris, France

¹⁰Department of Physics and Astronomy, Pevensey Building, University of Sussex, Brighton, BN1 9QH, UK

¹¹Department of Physics & Astronomy, University College London, Gower Street, London, WC1E 6BT, UK

¹²SLAC National Accelerator Laboratory, Menlo Park, CA 94025, USA

¹³Kavli Institute for Particle Astrophysics & Cosmology, P. O. Box 2450, Stanford University, Stanford, CA 94305, USA

¹⁴Centro de Investigaciones Energéticas, Medioambientales y Tecnológicas (CIEMAT), Madrid, Spain

¹⁵National Center for Supercomputing Applications, 1205 West Clark St., Urbana, IL 61801, USA

¹⁶Department of Astronomy, University of Illinois at Urbana-Champaign, 1002 W. Green Street, Urbana, IL 61801, USA

¹⁷Institut de Física d'Altes Energies (IFAE), The Barcelona Institute of Science and Technology, Campus UAB, 08193 Bellaterra (Barcelona) Spain

¹⁸INAF-Osservatorio Astronomico di Trieste, via G. B. Tiepolo 11, I-34143 Trieste, Italy

¹⁹Institute for Fundamental Physics of the Universe, Via Beirut 2, 34014 Trieste, Italy

²⁰Department of Physics, IIT Hyderabad, Kandi, Telangana 502285, India

²¹Jet Propulsion Laboratory, California Institute of Technology, 4800 Oak Grove Dr., Pasadena, CA 91109, USA

²²Department of Astronomy/Steward Observatory, University of Arizona, 933 North Cherry Avenue, Tucson, AZ 85721-0065, USA

²³Santa Cruz Institute for Particle Physics, Santa Cruz, CA 95064, USA

²⁴Institut d'Estudis Espacials de Catalunya (IEEC), 08034 Barcelona, Spain

²⁵Institute of Space Sciences (ICE, CSIC), Campus UAB, Carrer de Can Magrans, s/n, 08193 Barcelona, Spain

²⁶Department of Physics, Stanford University, 382 Via Pueblo Mall, Stanford, CA 94305, USA

²⁷Center for Cosmology and Astro-Particle Physics, The Ohio State University, Columbus, OH 43210, USA

²⁸Department of Physics, The Ohio State University, Columbus, OH 43210, USA

²⁹Center for Astrophysics | Harvard & Smithsonian, 60 Garden Street, Cambridge, MA 02138, USA

³⁰Physics Division, Lawrence Berkeley National Laboratory, Berkeley, CA 94720, USA

³¹Australian Astronomical Optics, Macquarie University, North Ryde, NSW 2113, Australia

³²Lowell Observatory, 1400 Mars Hill Rd, Flagstaff, AZ 86001, USA

³³Institució Catalana de Recerca i Estudis Avançats, E-08010 Barcelona, Spain

³⁴Institute of Astronomy, University of Cambridge, Madingley Road, Cambridge CB3 0HA, UK

³⁵Department of Astrophysical Sciences, Princeton University, Peyton Hall, Princeton, NJ 08544, USA

³⁶Department of Physics, University of Michigan, Ann Arbor, MI 48109, USA

³⁷School of Physics and Astronomy, University of Southampton, Southampton, SO17 1BJ, UK

³⁸Computer Science and Mathematics Division, Oak Ridge National Laboratory, Oak Ridge, TN 37831

³⁹Max Planck Institute for Extraterrestrial Physics, Giessenbachstrasse, 85748 Garching, Germany

⁴⁰Universitäts-Sternwarte, Fakultät für Physik, Ludwig-Maximilians Universität München, Scheinerstr. 1, 81679 München, Germany

ABSTRACT

We use a stacking method to study the radial light profiles of luminous red galaxies (LRGs) at redshift ~ 0.62 and ~ 0.25 , out to a radial range of 200 kpc. We do not find noticeable evolution of the profiles at the two redshifts. The LRG profiles appear to be well approximated by a single Sersic profile, although some excess light can be seen outside 60 kpc. We quantify the excess light by measuring the integrated flux and find that the excess is about 10% – a non-dominant but still nonnegligible component.

1. INTRODUCTION

Studies have found evidence that there exists an envelope distribution of diffuse stars around both early and late type galaxies (e.g., Sackett et al. 1994; Zibetti et al. 2004; Ibata et al. 2007; Tal & van Dokkum 2011; Trujillo & Bakos 2013; D’Souza et al. 2014; Duc et al. 2015), and an excessive amount around the central galaxies of galaxy clusters (e.g., Schombert 1986; Zibetti et al. 2005; Burke et al. 2015; Zhang et al. 2019). These diffuse stellar envelopes provide clues to how frequently galaxies interact, and how the galaxy interactions affect the galaxy stellar distribution (Font et al. 2011; Cooper et al. 2013; Elias et al. 2018). Unfortunately, their faintness and the effect of the observational point-spread function (PSF) mean that it is often difficult to quantify these diffuse stellar distributions accurately (de Jong 2008; Sandin 2014, 2015; Zackrisson et al. 2012), and their detection sparked debates.

We assess the diffuse stellar extent of luminous red galaxies (LRGs) and examine its redshift evolution between redshift ~ 0.25 and ~ 0.625 . We use a stacking method with optical images (Zhang et al. 2019) from the Dark Energy Survey (DES) to acquire high signal-to-noise LRG Surface Brightness (SB) measurements out to the radius of 200 kpc. We do not notice significant differences in the LRG profiles between redshift ~ 0.25 and ~ 0.625 . This analysis assumes a Λ CDM cosmology model with the Hubble parameter $h = 0.7$ and the matter density parameter $\Omega_m = 0.3$.

2. DATA AND METHODS

The LRG sample used in the analysis is selected from DES Year 1 data by the redMagic algorithm (Rozo, E. and Rykoff, E. S. et al. 2016), which is based on comparing galaxy colors to spectroscopic LRG samples. The algorithm delivers excellent galaxy photometric redshift estimation with a median scatter of $0.017(1+z)$, and provides the fiducial sample for the DES galaxy clustering analysis (Elvin-Poole et al. 2018). We study the LRGs in a low redshift range with photometric redshifts between 0.24 and 0.26 ($z \sim 0.25$), and in a high redshift range between 0.62 and 0.63 ($z \sim 0.625$). We analyze the r band SB profile of the $z \sim 0.25$ LRG sample, and the i profile of the $z \sim 0.625$ sample. The red-shifting from ~ 0.25 to ~ 0.625 places the DES r band at a similar rest-frame wavelength range with the i band, and thus eliminates the need of performing K-corrections when examining redshift evolution.

Our methods of preparing LRG images from DES Year 1 to 3 observations and measuring their SB profiles closely follow the procedures in Zhang et al. (2019). In total, we stack 201 LRGs at $z \sim 0.25$, and 1381 LRGs at $z \sim 0.625$. To reduce noise in the measurements, we also eliminate those LRGs close to bright stars or nearby galaxies as described in Zhang et al. (2019). The measured LRG SB profiles are fitted to Sersic models (Sérsic 1963) considering the stacked, extended DECam point spread function (PSF) averaged over DES Y3 observations. Figure 1 shows the stacked LRG r -band SB profile at $z \sim 0.25$ and the i -band profile at $z \sim 0.625$. The latter is corrected to $z \sim 0.25$ by the differences in luminosity distance moduli and angular-to-physical distance conversion.

3. RESULTS

We measure the LRG SB profiles with high S/N up to 200 kpc at both $z \sim 0.25$ and $z \sim 0.625$, and we do not notice significant evolution of the profiles between these redshifts, as they are consistent within 2σ . We fit a single Sersic model, although the data only seem to follow this model within ~ 60 kpc, and less well at $z \sim 0.625$. At $z \sim 0.25$, the LRG SB profile is fitted by a Sersic model with index $2.59_{-0.04}^{+0.05}$ and effective radius $8.8_{-0.1}^{+0.2}$ kpc. At $z \sim 0.625$, the fitted Sersic model has an index of $2.75_{-0.04}^{+0.03}$ and an effective radius of $11.5_{-0.5}^{+0.3}$ kpc. The model fitting results are not sensitive to PSF convolution. Beyond 60 kpc, both the $z \sim 0.25$ and $z \sim 0.625$ LRGs show an excess of light above the Sersic models.

We derive the integrated LRG fluxes within 200 kpc, which are similar at $z \sim 0.25$ and $z \sim 0.625$ (corrected to the observer frame at $z \sim 0.25$) with values of 17.96 ± 0.07 mag and 17.93 ± 0.03 mag respectively. The integrated flux in the annulus between radius 60 and 200 kpc makes up 11.6% of the total LRG flux within 200 kpc at $z \sim 0.25$, or 9.7% of the total flux at $z \sim 0.625$. In terms of the best-fitting Sersic models, the fluxes contained in the actual measurements but not in the models make up 10.0% and 5.8% of the total fluxes within 200 kpc at $z \sim 0.25$ and $z \sim 0.625$ respectively. We conclude that the extended light beyond 60 kpc, or the excess light not modeled by a single Sersic model, is not dominant but nevertheless still a nonnegligible LRG component.

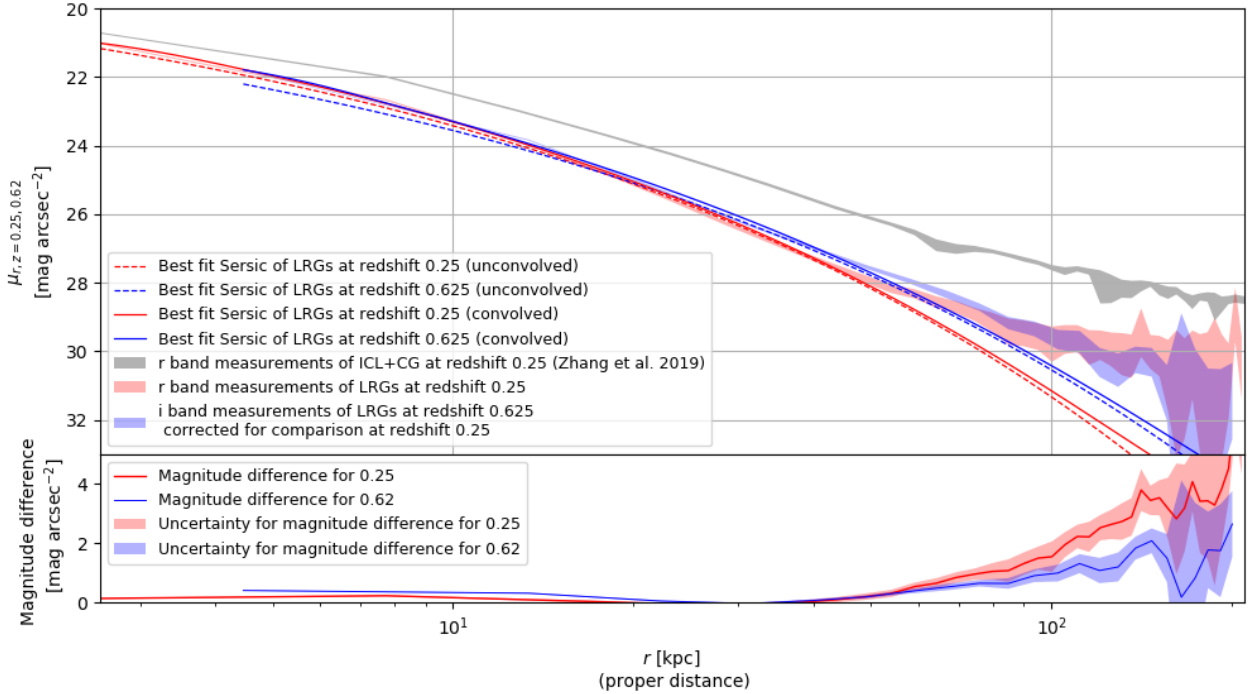


Figure 1. The upper panel shows the measured LRG SB profiles at redshift ~ 0.25 and ~ 0.625 . The blue and red shaded regions indicate the corresponding uncertainties. The solid and dotted lines show the same best-fit Sersic models with and without including the effect of PSF. The lower panel shows the residual between the data and the best-fit models. For comparison, we also overplot the intra-cluster light and central galaxy (ICL+CG) measurements at $z \sim 0.25$ in Zhang et al. (2019) as the grey shaded region.

A similar stacking analysis of LRGs has been reported in Tal & van Dokkum (2011) using SDSS data. They find that a Sersic model with $n = 5.8$ and $r_e = 13.6$ kpc fits the LRG profile well at $z \sim 0.34$ to ~ 100 kpc, which is different from our results. We suspect that the image processing methods, especially in terms of sky background estimations (Bernstein et al. 2017; Blanton et al. 2011), may have played a role. We also consider how our LRG measurements differ from the intra-cluster light and central galaxy (ICL+CG) measurements at $z \sim 0.25$ in Zhang et al. (2019). Unsurprisingly, the ICL+CG profile is brighter and its shape is more extended than the LRGs, as anticipated by the inside-out galaxy formation scenario in which CG starts out as a luminous compact galaxy and grows by merging in its peripheral regions (e.g., Laporte et al. 2013; Ragone-Figueroa et al. 2018). We have also analyzed the LRG $g-r$ ($z \sim 0.25$) and $r-i$ ($z \sim 0.625$) colors in our analysis, but unfortunately do not have enough signal-to-noise outside 20 kpc to draw robust conclusions.

This note is prepared under the DES publication guidelines¹. A standard DES acknowledgment applies.

REFERENCES

- Bernstein, G. M., Abbott, T. M. C., Desai, S., et al. 2017, PASP, 129, 114502
- Blanton, M. R., Kazin, E., Muna, D., Weaver, B. A., & Price-Whelan, A. 2011, AJ, 142, 31
- Burke, C., Hilton, M., & Collins, C. 2015, MNRAS, 449, 2353
- Cooper, A. P., D’Souza, R., Kauffmann, G., et al. 2013, MNRAS, 434, 3348
- de Jong, R. S. 2008, MNRAS, 388, 1521
- D’Souza, R., Kauffman, G., Wang, J., & Vegetti, S. 2014, MNRAS, 443, 1433
- Duc, P.-A., Cuillandre, J.-C., Karabal, E., et al. 2015, MNRAS, 446, 120
- Elias, L. M., Sales, L. V., Creasey, P., et al. 2018, MNRAS, 479, 4004
- Elvin-Poole, J., Crocce, M., Ross, A. J., et al. 2018, PhRvD, 98, 042006

¹ <http://dbweb5.fnal.gov:8080/DESPub/app/PB/pub/pbpublished>

- Font, A. S., McCarthy, I. G., Crain, R. A., et al. 2011, MNRAS, 416, 2802
- Ibata, R., Martin, N. F., Irwin, M., et al. 2007, ApJ, 671, 1591
- Laporte, C. F. P., White, S. D. M., Naab, T., & Gao, L. 2013, MNRAS, 435, 901
- Ragone-Figueroa, C., Granato, G. L., Ferraro, M. E., et al. 2018, MNRAS, 479, 1125
- Rozo, E. and Rykoff, E. S., Abate, A., Bonnett, C., et al. 2016, MNRAS, 461, 1431
- Sackett, P. D., Morrisoni, H. L., Harding, P., & Boroson, T. A. 1994, Nature, 370, 441
- Sandin, C. 2014, A&A, 567, A97
- . 2015, A&A, 577, A106
- Schombert, J. M. 1986, ApJS, 60, 603
- Sérsic, J. L. 1963, Boletín de la Asociación Argentina de Astronomía La Plata Argentina, 6, 41
- Tal, T., & van Dokkum, P. G. 2011, Astrophysical Journal - ASTROPHYS J, 731
- Trujillo, I., & Bakos, J. 2013, MNRAS, 431, 1121
- Zackrisson, E., de Jong, R. S., & Micheva, G. 2012, MNRAS, 421, 190
- Zhang, Y., Yanny, B., Palmese, A., et al. 2019, ApJ, 874, 165
- Zibetti, S., White, S. D. M., & Brinkmann, J. 2004, MNRAS, 347, 556
- Zibetti, S., White, S. D. M., Schneider, D. P., & Brinkmann, J. 2005, MNRAS, 358, 949